Shell ultrastructure of the Taxodont Pelecypod Anadara notabilis (Röding)

Autor(en): **Wise, Sherwood W.**

Objekttyp: **Article**

Zeitschrift: **Eclogae Geologicae Helvetiae**

Band (Jahr): **64 (1971)**

Heft 1

PDF erstellt am: **13.09.2024**

Persistenter Link: https://doi.org/10.5169/seals-163965

Eclogae geol. Helv.	Vol. 64/1	Pages 1–12	3 figures in the text and 9 plates (I-IX)	Basle, April 1971

Shell Ultrastructure of the Taxodont Pelecypod *Anadara notabilis* (RÖDING)

By SHERWOOD W. WISE JR.

Geologisches Institut, Eidgenössische Technische Hochschule,
formerly Department of Geology, University of Illinois, Urbana

ABSTRACT

The shell structure of the pelecypod *Anadara notabilis* (RÖDING) (Recent: Bahamas) has been studied by correlated light microscopy, transmission electron microscopy and scanning electron microscopy of polished and etched sections, fracture surfaces and developmental surfaces. The shell is composed of two structural layers: an outer crossed lamellar layer and an inner layer of complex crossed lamellar structure. The crossed lamellar layer consists of first, second and third order lamels; the latter are lath shaped units approximately 0.4–0.5 μ wide, 0.15 μ thick and at least 7.3 μ long. The complex crossed lamellar layer is composed of aragonite strands deposited in either a "lineated" or "cross-matted" pattern. Tubules are emplaced in the endostracum just inside the pallial line and penetrate all shell layers. Tubule openings are confined to parallel grooves which run from the pallial line toward the beak of the shell. Near the pallial line the grooves are separated by ridges composed of myostracum which mark attachment sites of pallial muscles. The myostracum which forms the ridges has a prismatic structure identical to that of adductor myostracum and similarly is covered by a thick organic membrane.

Introduction

Although most studies of molluscan shell ultrastructure concern the nacreous and prismatic layers, the most common and characteristic of all shell structures is the crossed lamellar layer which occurs in four of the six classes of molluscs: the pelecypods, gastropods, scaphopods and polyplacophorids (BØGGILD 1930). In fourteen families of pelecypods, crossed lamellar structure occurs as an outer shell layer in combination with an inner layer having complex crossed lamellar structure[1]) (OBERLING 1964). These fourteen families comprise most of the taxa assigned to the "complex-lamellar" shell structure group, one of the three major divisions into which OBERLING (1964) divided pelecypods on the basis of shell microstructure. Although these families are placed in a single group under the classificatory scheme outlined by OBERLING, they are split among several different independently evolving lineages according to the phylogenetic schemes of DALL and DOUVILLÉ (see NEWELL 1969, Fig. 101 and Table 1). If the schemes of DALL and DOUVILLÉ represent a reasonably close approximation of the true evolutionary development of these lineages, it would

[1]) Complex structure of OBERLING (1964) and KOBAYASHI (1964a) (see discussion of these terms by TAYLOR et al. 1969, p.47).

appear that crossed lamellar structure evolved independently in each of several different branches of the Bivalvia (OBERLING 1964, p. 35). If this is so, the development of crossed lamellar structure in these various groups represents a classic example of parallel evolution, a phenomenon not uncommon in molluscs.

If it is assumed that crossed lamellar structure did develop independently in several different lineages of the "complex-lamellar" group, it would not be surprising to find, at the ultrastructure level, subtle differences in construction which would betray a polyphyletic origin for this shell fabric. Unfortunately, outside of the work of KOBAYASHI and his associates (KOBAYASHI 1964a, 1964b; KOBAYASHI and KAMIYA 1968) and recent investigations by TAYLOR, KENNEDY and HALL (TAYLOR and KENNEDY 1969; TAYLOR et al. 1969), few studies have dealt with the ultra-architecture of shells having a crossed lamellar or a complex crossed lamellar layer. The quantity of data presented in these studies is not sufficient to allow meaningful comparisons to be made between the various pelecypod groups mentioned above or, on a larger scale, between pelecypods and other Classes of molluscs. There is presently a clear need for additional highly detailed studies of individual taxa which possess crossed lamellar and/or complex crossed lamellar structure. Because both layers are well developed in the clam *Anadara notabilis* (RÖDING), this arc shell has been chosen for study by transmission and scanning electron microscopy. The purpose of the study is to illustrate the fine structures of the shell layers and their relationship to the general morphology of the shell.

Materials and methods

Specimens of *Anadara notabilis* and *Arca zebra* were collected live at water depths of approximately one to two meters in Bimini Lagoon, Bimini, Bahamas. Soft parts were removed at the time of collection.

All micrographs in this report are scanning electron micrographs except for those specifically designated otherwise. In previous reports dealing with molluscan shell material, detailed instructions have been given for preparing 1. cellulose acetate peels of polished and etched sections, 2. light micrographs of acetate peels, 3. oriented two-step carbon replicas of etched sections, and 4. scanning electron micrographs of etched sections, fracture sections, and developmental growth surfaces (WISE and HAY 1968a, 1968b; WISE 1970). These procedures will not be redescribed here.

Results and discussion

The exterior of the shell of *A. notabilis* is covered by a bristly periostracum (Pl. I, Fig. 1). Developmental "growth" surfaces of the principal shell layers are visible on the interior (Pl. I, Fig. 2). The growth surface of the crossed lamellar layer (*CL*) covers the hinge and the area ventral to the pallial line (arrow *PL*). Adjacent to the pallial line, this growth surface is flat and smooth (lighter area of *CL*, Pl. I, Fig. 2), but becomes deeply folded along the ventral margin where the ribs are formed (darker colored portion of *CL*, Fig. 2). The complex crossed lamellar layer (*CPX*) is deposited over the interior of the shell inside the pallial line except in the areas covered by myos-

tracum. In *A. notabilis*, myostracum is secreted 1. at sites along the pallial line where the mantle is attached to the shell, and 2. at either end of the hinge where the adductor muscles are attached (labled *M* in Pl. I, Fig. 2). The relative positions of the complex and crossed lamellar layers are shown diagrammatically in the radial cross section (Pl. I, Fig. 3) which was cut along the white line indicated in Figure 2. The complex crossed lamellar layer is deposited on top of the crossed lamellar layer and lies proximal to it. The intricate structure within the hinge area of *Anadara* is described by MANO and OMORI (1969) and will not be discussed here. As indicated in Plate I, Figure 3, all micrographs and figures of shell layers in this report (with the exception of Pl. IV, Fig. 5 and 6) are oriented with the proximal (inner) layer at the top of the figure in its natural depositional position.

Crossed lamellar structure

The gross morphology of crossed lamellar structure is shown by a radial fracture (Pl. I, Fig. 4) which intersects the inner surface of the shell (*IS*), a thin myostracum deposit (*M*), and a portion of the much thicker crossed lamellar layer (*CL*). The large vertical sheet-like units below the myostracum are the first order lamels of the crossed lamellar layer (BØGGILD 1930). These units are composed of smaller units called second order lamels which BØGGILD (1930, p. 251) illustrated in his interpretative diagram of crossed lamellar structure (Textfig. 1). His figure shows three first order lamels, each composed of lath shaped second order lamels, which, in adjacent first order lamels, are inclined in opposite directions. The second order lamels cross at an angle of about 98°; however, this value may vary considerably in different species. Although previous interpretations of crossed lamellar structure are confusing and conflicting (MACCLINTOCK [1967] presents an excellent summary of these), BØGGILD's

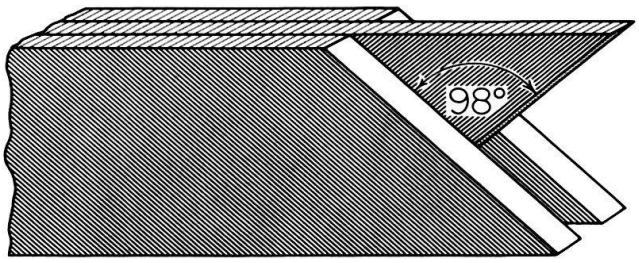

Fig. 1. Diagrammatic representation of crossed lamellar structure (after BØGGILD 1930).

representation has served as a reliable model for subsequent light microscopic studies (NEWELL 1937; TRUEMAN 1942; REYNE 1951; OBERLING 1964; MACCLINTOCK 1967). BØGGILD's model has been further refined by KOBAYASHI (1964a, 1964b) on the basis of observations made using the transmission electron microscope.

Plate I, Figure 5, is a view of the inner shell surface showing the pallial line (arrow *PL*) which marks the boundary between the inner layer (upper portion of figure) and the crossed lamellar layer (lower portion). Beginning at the pallial line, a series of grooves punctuated by tubule openings runs across the inner surface of the shell

toward the dorsum (to be discussed later). As indicated in Plate I, Figure 4, the first order lamels are oriented perpendicular to the growth surface of the crossed lamellar layer. Their traces on the inner surface (lower portion of Pl. I, Fig. 5) appear as long narrow streaks which run approximately parallel to the ventral margin (according to BØGGILD's terminology, "concentrically") and taper out or bifurcate at each end.

Transmission electron micrographs of carbon replicas have revealed the traces of second order lamels on the growth surface of the crossed lamellar layer of *Barbatia* (KOBAYASHI 1964a, Pl. II, Fig. 5). Light etching of the growth surface, however, reveals the presence of finer units which KOBAYASHI (1964a) named "third order lamels". Plate I, Figure 6, shows four adjacent first order lamels composed of innumerable third order lamels which, in adjacent first order lamels, incline in opposite directions. A view at higher magnification of the boundary between two adjacent first order lamels (Pl. I, Fig. 7) shows that the third order lamels of each are inclined to the growth surface at the same angle, but dip in opposite directions.

KOBAYASHI (1964b, p. 6, Textfig. 8) depicted third order lamels as lath shaped elements laid side by side like planks in a wooden floor to form the second order lamels. Transmission electron micrographs of etched sections polished parallel to the growth surface support this interpretation. In Plate II, Figure 1, the third order lamels appear to be fitted together into continuous sheets. The linear boundaries etched in the second order lamels suggest that the average width of the third order lamels is 0.4–0.5 μ. KOBAYASHI (1964a, p. 300) also found this width to be 0.5 μ in *Barbatia*.

Organic matrices have been observed interleaved between the second order lamels (see MACCLINTOCK 1967, p. 24; TAYLOR et al. 1969, p. 46) and those from the arc

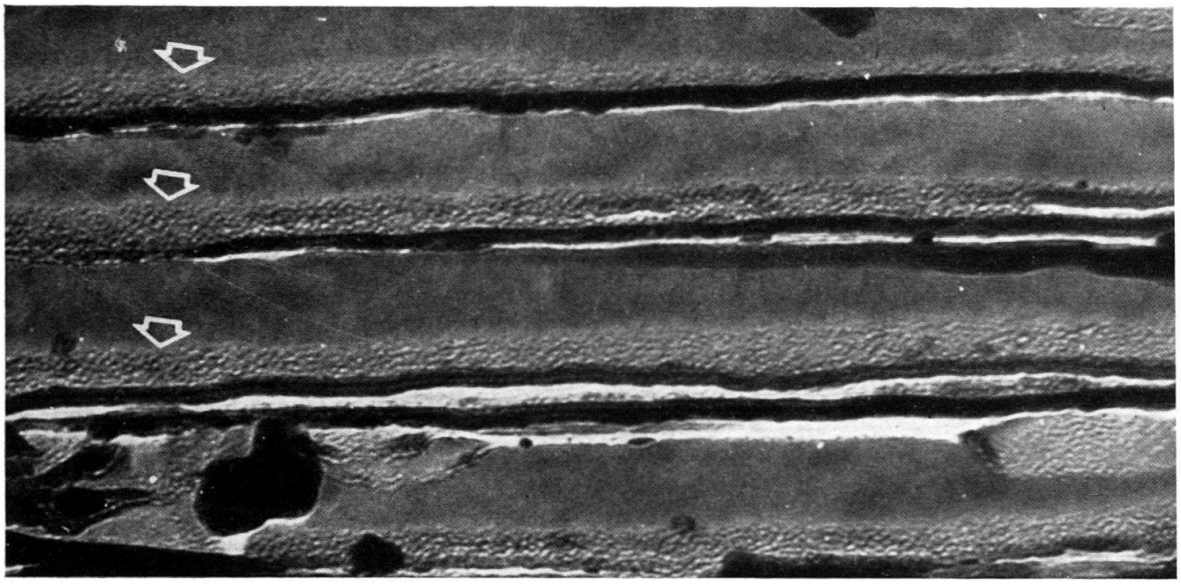

Fig. 2. *Arca zebra* SWAINSON. Transmission electron micrograph of an etched polished section through the crossed lamellar layer reveals lacy organic matrices (arrows) interleaved between second order lamels. Trabecular cords of the organic membranes form the finely reticulate "pelecypod" pattern described by GRÉGOIRE et al. (1950, 1955), 60,000 ×.

shell *Arca zebra* SWAINSON (Textfig. 2) exhibit the same "tight pelecypod" pattern that GRÉGOIRE et al. (1950, 1955) observed in the nacreous layer of lamellibranchs (see also GRÉGOIRE 1967). It has not been determined whether organic matrices partition the second order lamels into third order lamels. However, the existence of third order lamels is indicated by fractures as well as by etch patterns; both tend to parallel the lengths of the second order lamels. Plate II, Figure 2, shows the intersection of a radial fracture and the inner shell surface. The fracture displays the broken ends of six first order lamels and the inclination of the finer elements. This configuration nearly duplicates that shown in BØGGILD's diagram (Textfig. 1). Also, fractures in the plane of the second order lamels are parallel to their lengths. On the inner surface (left portion of Pl. II, Fig. 2), slight depressions outline the boundaries between first order lamels.

The true thicknesses of the second and third order lamels are the same, and can only be measured on a section parallel to the boundary between two adjacent first order lamels. Plate III, Figure 1, is a transmission electron micrograph of such a section, and the second order lamels are seen in longitudinal cross section. They are about 0.15 μ thick and at least 7.3 μ long. These observations confirm KOBAYASHI's interpretation of the submicroscopic structure of the crossed lamellar layer in pelecypods which is illustrated in parts *A–C* of Texfigure 3. The three orders of structure are: *A* first order lamels; *B* second order lamels; *C* third order lamels. In pelecypods, the smallest dimensions of the third order lamels (0.15 μ) correspond to the thicknesses of the second order lamels. In gastropods, however, MACCLINTOCK (1967, p. 19) measured the thicknesses of second order lamels at 1.0, 1.3 and 1.6 μ, and found the widths of third order lamels to be about 0.5 μ. Therefore, in his reconstruction (parts *D*, *E* and *F*, Texfig. 3) the smallest dimensions of the third order lamels do not coincide with the thicknesses of the second order lamels. Although his values were obtained by light microscopy and cannot be as accurate as measurements based on electron micrographs, the arrangement of his third order lamels is similar to those figured by NATHUSIUS-KÖNIGSBORN (1877, Pl. 4, Fig. 23) from observations of the gastropod *Strombus*. This at least suggests the possibility that there may be a fundamental difference in the organization of third order lamels between pelecypods and some gastropods. Further electron microscope investigations are needed to clarify this point.

Plate III, Figure 2, indicates that fractures through cross lamellar structure tend to follow the planes of weakness offered by the trend of the second order lamels. Indeed fractures may follow preferentially the plane of weakness offered by one set of second order lamels while truncating the second set at right angles (Pl. III, Fig. 2). Occasional interruptions in this pattern occur where the fracture truncates both sets of lamels and follows zones of weakness apparently induced by the presence of tubules (lower portion of figure). In a view perpendicular to the fracture surface (Pl. III, Fig. 3), the second order lamels appear as lath shaped stubs in the truncated set and as strips of veneer in the set fractured parallel to their face. The organic matrices between the second order lamels bond them together in a tightly knit structure resembling plywood.

The first order lamels of *A. notabilis* are parallel to the ventral margin and perpendicular to the ribs of the shell (Pl. I, Fig. 2 and 5). Therefore, radial cross sections (those parallel to the ribs) intersect the first order lamels at right angles. If BØGGILD's

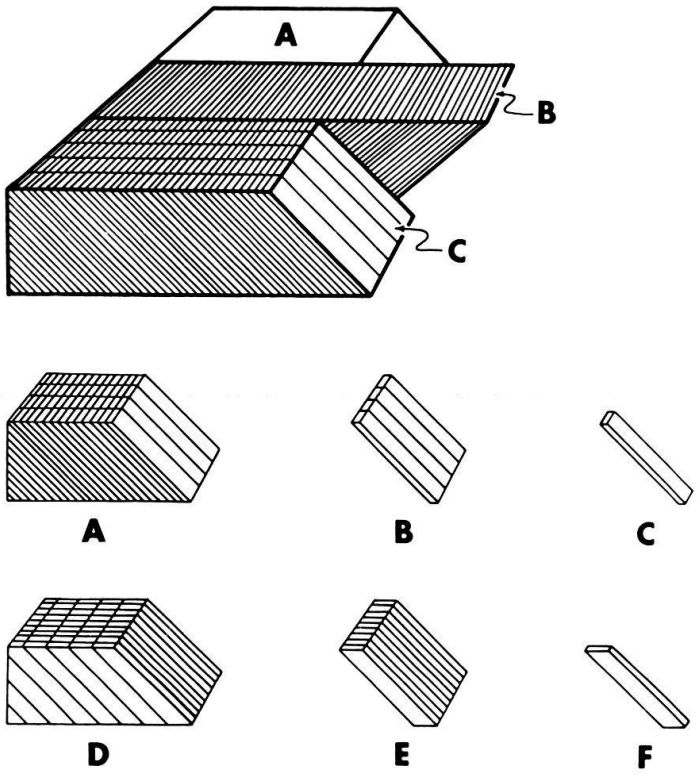

Fig. 3. Diagrammatic representation of crossed lamellar structure in pelecypods and gastropods. Units in pelecypods are: *A* first order lamels; *B* second order lamels; *C* third order lamels (after KOBAYASHI 1964b). *D*, *E* and *F* represent first, second and third order lamels in gastropods studied by MACCLINTOCK (after MACCLINTOCK 1967).

reconstruction is correct, second order lamels should appear as parallel horizontat lines on radial cross sections (as on radial section *R* of Pl. IV, Fig. 1). The lighl micrograph of a radial section (Pl. IV, Fig. 2) reveals the relationship predicted by the diagram in Plate IV, Figure 1. The vertical units are first order lamels, and the parallel horizontal lines are the heavily etched traces of second order lamels.

Plate IV, Figure 3, is an acetate peel of a radial section through the entire thickness of the shell showing a thin complex crossed lamellar layer overlying the crossed lamellar layer. In the proximal half of the latter, the first order lamels are straight, parallel, and nearly vertical to the inner surface of the shell. All micrographs in the preceding figures were taken in this area of the shell. They betray the presence of obvious planes of weakness at the boundaries between first order lamels (see Pl. I, Fig. 4). To counteract this, in the distal half of the layer where the ribs are formed, the first order lamels are reclined to a subhorizontal orientation (they are, nevertheless, always perpendicular to the growth lines [white traces, left portion of Fig. 3]). Furthermore, where the straight parallel first order lamels of the proximal sublayer pass directly into a rib (right center of Pl. IV, Fig. 3; upper half of Pl. IV, Fig. 4), they change directions abruptly, bifurcate, ramify, anastomose, and break up into many small, loosely connected units which are tightly woven together to eliminate all possible planes of weakness and to add strength to the shell.

Although the structure of the crossed lamellar layer is vastly more complicated in the ribbed portion of the shell, the same modules of construction are used throughout both sublayers. A fracture through the ribs (Pl. IV, Fig. 5 and 6; proximal direction toward bottom) reveals the regular alternation in the direction of inclination of successive second order lamels. In Plate IV, Figure 5, the horizontal first order lamels follow the contour of the ribs.

Tubules

Among the most interesting features of the *Anadara* shell are the tubulate grooves which run from the pallial line toward the beak of the shell (Pl. I, Fig. 5). The tubules are formed secondarily in the crossed lamellar layer and are emplaced just behind the pallial line (Pl. V, Fig. 1). Several may be formed at once, sometimes in a line or chain (note tubules along pallial line in Pl. V, Fig. 1). The tubules penetrate all the way through the shell as straight borings which incline toward the ventral margin at about a 70° angle (Pl. V, Fig. 2 and 3). They always cross the first order lamels at an angle which is quite variable because of the change in orientation of the lamels in different parts of the layer. The tubules remain open as the complex crossed lamellar layer is deposited around them, the result being that they assume an orientation perpendicular to the inner layer (Pl. V, Fig. 3). This accounts for their abrupt change in direction at the crossed lamellar/complex crossed lamellar layer boundary.

Tubules were first described by CARPENTER in 1844 and were referred to as *Kanäle* by German investigators (EHRENBAUM 1885). Ignored by BØGGILD (1930) and most other investigators during the first half of the twentieth century, they were poorly known until OBERLING (1955, 1964) plotted their occurrence in many families of pelecypods. Tubules have subsequently been described by OMORI et al. (1962); OMORI and KOBAYASHI (1963); KOBAYASHI (1964); KILHAM (1969); WISE (1969 b); TAYLOR and KENNEDY (1969); TAYLOR et al. (1969).

In some pelecypods tubules apparently form contemporaneously with the shell layer they penetrate (IHERING 1874); however, in arc shells, they form after the crossed lamellar layer is deposited (OBERLING 1964, p. 18). They are not visible on the growth surface of that layer and only occur within the pallial line. Although they must be formed by resorption, the exact mechanism by which this occurs is unknown. It has been assumed that some kind of an organic material fills the tubules during the life of the animal (OMORI and KOBAYASHI 1963, p. 279), and SHIBATA (1965) has reported conchiolin in tubules of *Glycymeris*. In decalcified sections TAYLOR and KENNEDY (1969, p. 396) found "only the ambiguous traces of mantle extensions into these holes". Material used in the present study was not fixed and had been stored in a dry atmosphere environment for three years before examination. No material was observed in tubules exposed by fracture; however, on the inner surface of the shell, desiccated strands of organic matter (possible protuberances of mantle material) were seen occasionally in tubule openings (Pl. VI, Fig. 1 and 2). Study of properly fixed material may provide more information on this problem.

Complex crossed lamellar structure

The term "complex crossed lamellar structure" is applied to a variety of structural configurations in gastropods and pelecypods which are thought to be composed of units which correspond to the second order lamels of crossed lamellar structure (TAYLOR et al. 1969, p. 47). Several varieties of this structure are discussed by MACCLINTOCK (1967), TAYLOR and KENNEDY (1969), and TAYLOR et al. (1969). In a number of cases (including that of *A. notabilis*, present study), the supposed "crossed" nature of the second order lamels of complex crossed lamellar structure is not readily apparent, particularly in the ventral region of the shell; however, the total amount of variation in configurations classed as "complex crossed lamellar structure" is not well enough known to permit a meaningful revision or redefinition of the structure at the present time. Nevertheless, in view of the variety of architectures already demonstrated for this shell layer, it may be conjectured that, among major groups of molluscs, this should be a particularly fruitful structure to examine for subtle differences in ultrastructure which may have taxonomic importance.

Plate VI, Figure 3, is a view of the inner shell surface looking from the beak region toward the pallial line and the growth surface of the crossed lamellar layer (*CL*, upper part of figure). The tubulate grooves *(T)* are parallel and separated by ridges which OBERLING (1964, p. 52) conjectured were sites of muscle attachment. These ridges are composed of myostracum (*M*) (evidence for this will be given later). The grooves are marked by bumps, some of which coincide with tubule openings (Pl. VI, Fig. 4). Within the grooves, material forming the complex crossed lamellar layer is deposited in the form of long strands of aragonite aligned in a linear pattern subparallel to the length of the grooves. These strands correspond to the "ridges" observed by TAYLOR et al. on the inner surface of *Anadara antiquata* and *Barbatia fusca* (TAYLOR et al. 1969, explanations for Pl. 22, Fig. 1 and 2). About $^1/_4$–1 mm from the pallial line, complex crossed lamellar material begins to be deposited beyond the margins of the grooves, lapping over the surface of the ridges and eventually covering them (Pl. VI, Fig. 3 and 5). Figure 5 is a close-up of the white rectangle in Figure 3 showing the dorsal termination of a myostracum ridge (*M*). Stands of complex crossed lamellar material are deposited over the ridge in a cross-matted pattern (*CM*) which contrasts sharply with the smooth lineated pattern (*L*) in the groove (Pl. VI, Fig. 6). As shown most clearly in the cross-matted area (Pl. VI, Fig. 6), the aragonite strands are elongate units about 1–3 μ wide which have round cross sections and pointed terminations. The strands are composed of small elongate crystals which, in some species (and possibly under certain ecological conditions), may be lath shaped with euhedral terminations (TAYLOR et al. 1969, Pl. 21, Fig. 4; Pl. 22, Fig. 1).

Within the grooves, the smooth-flowing fibrous appearance of the lineated pattern is seen both on the growth surface and in radial fracture sections. The radial fracture in Plate VII, Figure 1, intersects the growth surface (top third of figure) and the thin layer of lineated complex crossed lamellar material (*CPX*) which overlies vertical first order lamels of the crossed lamellar layer (*CL*).

Near the pallial line, the grooves are deep and visible to the naked eye (see area in Pl. I, Fig. 2, near the arrow marked *PL*); however, toward the beak the distinction

between groove and ridge is eventually lost as the latter are covered by thicker and thicker accretions of complex crossed lamellar material. Even closer to the beak, the tubule openings are no longer confined to rows, but are scattered over the inner surface at random.

Myostracum

Tubules, into which protuberances of the mantle are thought to project, indicate an intimate association of mantle to shell. The mantle is also attached along the pallial line and presumably along the myostracum ridges. Plate VII, Figure 2, shows a transverse fracture near the pallial line which cuts through a myostracum ridge (center) and two grooves (on either side of ridge), and exposes the crossed lamellar layer below. A second ridge is seen in the background. As described by light microscopists, the internal structure of myostracum (OBERLING 1955, p. 128) is distinctly prismatic and appears bright and transparent in the light microscope. For this reason it has been referred to as the *durchsichtige prismatische Perlmutterschicht* (NATHUSIUS-KÖNIGSBORN 1877), the *helle Schicht* (TULLBERG 1882; SCHMIDT 1923), and the "pellucid layer" (KADO 1953; KOBAYASHI 1964b). It has also been called the "hypostracum" (THIELE 1893; JAMESON 1912; NEWELL 1937). The fractograph in Plate VIII, Figure 1, reveals the entire thickness of the myostracum ridge shown in the center of Plate V, Figure 2. The prismatic elements are typically wedge-shaped, have irregular boundaries, and exhibit smooth concoidal fractures in cross section.

In *Nautilus* adductor myostracum deposits are separated from the secreting epithelium by a thick organic membrane to which the myo-adhesive epithelial cells are firmly attached (MUTVIE 1964, p. 245). A similar membrane about $^1/_2$–1 μ thick covers the myostracum of the ridges of *Anadara* (Pl. VIII, Fig. 2). The arrow in the center of Figure 2 points to a crack running through the mat-like membrane. To the left of the arrow, a prism of myostracum is suspended from the edge of the mat. In every other respect the myostracum of the ridges resembles the prismatic structure of the adductor myostracum (seen in Pl. VIII, Fig. 3). The prismatic elements of both are perpendicular to the inner surface of the shell. Therefore, the myostracum ridges represent attachment sites of the pallial muscles.

In cellulose acetate peels enlarged photographically, the myostracum of the ridges appears dark against the light background of the complex crossed lamellar layer both in radial section (arrow, Pl. IV, Fig. 3) and transverse section (arrows, Pl. VIII, Fig. 4). In the crossed lamellar layer of the transverse section (Fig. 4 above) are portions of two ribs (*R*) and a rib interspace (*I*). Seven myostracum ridges (arrows, Fig. 4) occur within the corresponding interval in the complex crossed lamellar layer indicating that approximately four to five ridges are present on the inner surface for every rib and rib interspace on the outer layer.

Plate IX, Figure 1, is a polished and etched radial section taken halfway between the pallial line and the beak of the shell (arrow *V* indicates ventral direction). The complex crossed lamellar layer (*CPX*) is thicker in this portion of the shell and completely covers a myostracum ridge (*M*) which overlies the crossed lamellar layer (*CL*). Within the complex crossed lamellar layer the lineated pattern is dominant and uniform over large areas (Pl. IX, Fig. 2) although local variations do occur (Pl. IX, Fig. 3). The change in tone in the complex crossed lamellar layer seen in Plate IX, Figure 1,

from dark (below) to light (above) is caused by a general change in the orientation of the aragonite strands. In etched section the myostracum exhibits characteristic wedge-shaped prisms (Pl. IX, Fig. 4) The myostracum in Plate IX, Figure 1, is built on a substructure of units which are inclined toward the dorsum (to the right).This sublayer has not been observed before; however, stereomicrographs (Pl. IX, Fig. 5) indicate that the prisms arise directly from the units of the sublayer. The heavy etching of the section has hollowed out some of the prisms, but has also delineated groups of crystals in the complex crossed lamellar layer above. Many of these are oriented in different directions and may indicate cross-matted structure.

The present study is an account of three shell structures observed in a single pelecypod species. As the work of KOBAYASHI (1964a) and TAYLOR et al. (1969) indicates, some differences are to be expected in the arrangement and configuration of these structures in other taxa (even within the same genus). As more detailed studies of single taxa become available, a clearer picture should emerge of the variations these structures exhibit within the phylum. Only then can more meaningful definitions be given to those structures which are now poorly understood. Studies most helpful toward achieving this goal are those which, as far as possible, relate 1. the three-dimensional orientation of the micro-structure described to the gross morphology of the shell, and 2. the configurations of the developmental growth surface to the internal structure of the layer.

Acknowledgments

This report is a portion of a thesis submitted in partial fulfillment of the requirements for the degree of Doctor of Philosophy in Geology at the University of Illinois at Urbana. The paper was presented in abstract form at the 81st Annual Meeting (Mexico City) of the Geological Society of America (WISE 1969 a). Grateful acknowledgment is made to Professor William W. Hay, who introduced the writer to electron microscopy and the study of skeletal ultrastructure, aided in securing equipment, and made numerous helpful suggestions throughout the study. Dr. Hanspeter Mohler provided valuable instruction and assistance during the early phases of the transmission electron microscope investigation which was carried out at the Central Electron Microscope Laboratory of the University of Illinois and on a JEM-7 Electron Microscope in the Geology Department of the University of Illinois (provided by National Science Foundation grant GB-3522 and the University Reseach Board). The Cambridge Mark IIA Scanning Electron Microscope used in the study is housed at the Central Electron Microscope Laboratory of the University of Illinois, and was purchased with funds from the National Science Foundation (NSF-GA-1239), the Public Health Service (PH-FR-07030) and the University Research Board. I thank Dr. B. Vincent Hall, Director of the Central Electron Microscope Laboratory, Mr. Lee Dryer, Dr. Richard Harmer and Mrs. Olive Stayton for their aid and assistance.

Mrs. Cynthia Curtiss Wise typed the manuscript, and Mr. Leslie R. Lewis assisted in drafting the figures. Funds for the collection of specimens at the Lerner Marine Laboratory, Bimini, Bahamas, were provided in part by the Department of Geology, University of Illinois and by National Science Foundation grants NSF-GP-1991 and NSF-FP-5056 to William W. Hay. I thank Robert Mathewson, Director of the Lerner Marine Laboratory, for his cooperation and assistance.

REFERENCES

BØGGILD, O.B. (1930): *The Shell Structure of the Mollusks*. K.Danske Vidensk. Selsk. Skr., Naturv. og math.Afd. [Ser.9] *2*, 231–325.

CARPENTER, W. (1844): *On the Microscopic Structure of Shells*. Br.Ass.Adv.Sci.Rep. (for 1844), p. 1–24.

EHRENBAUM, E. VON (1885): *Untersuchungen über die Struktur und Bildung der Schale der in der Kieler Bucht häufig vorkommenden Muscheln*. Z.wiss.Zool., Leipzig *41*, 1–47.

GRÉGOIRE, CH. (1967): *Sur la Structure des matrices organiques des coquilles de mollusques*. Biol.Rev. *42*, 653–688.

GRÉGOIRE, CH., DUCHÂTEAU, GH., and FLORKIN, M. (1950): *Structure étudiée au microsope électronique, des nacres déclacifiées de mollusques (gastéropods, lamellibranches, et céphalopodes)*. Archs int.Physiol.*58*, 117–120.

– (1955): *La trame protidique des nacres et des perles*. Annls Inst.océanogr.*31*, 1–36.

IHERING, H. VON (1874): *Über die Entwicklungsgeschichte der Najaden*. Naturf.Ges.Leipzig, Sitzungsber.*2*, 3–6.

JAMESON, H.L. (1912): *Studies on Pearl-Oysters and Pearls. I. The Structure of the Shell and Pearls of the Ceylon Pearl-Oyster (Margaritifera vulgaris Schumacher): with an Examination of the Cestode Theory of Pearl-Production*. Proc.zool.Soc.Lond. [Ser.B] *22*, 260–358.

KADO, Y. (1953): *On the Scheme of the Structure of Lamellibranchs*. J.Sci.Hiroshima Univ. [Ser.B, div.1] *14*, 243–254.

KILHAM, S.S. (1969): *Skeletal Structures in Deep-Sea Molluscs*. Geol.Soc.Am., *Abstracts with Programs for 1969*, Part 4, p.42.

KOBAYASHI, I. (1964a): *Microscopical Observations on the Shell Structure of Bivalvia*. Part.I. *Barbatia obtusoides (Nyst.)* Sci.Rep.Tokyo Kyoiku Daig. [Sec.C] *8*, 295–301.

– (1964b): *Introduction to the Shell Structure of Bivalvian Molluscs*. Earth Sci. (Chikyu Kagaku) *73*, 1–12.

KOBAYASHI, I., and KAMIYA, H. (1968): *Microscopic Observations on the Shell Structure of Bivalves*. Part III. Genus *Anadara*. J.geol.Soc.Japan (Jour.Nihon Chishitsu Gakkai) *74*, 351–362.

MACCLINTOCK, C. (1967): *Shell Structure of Patelloid and Bellerophontoid Gastropods (Mollusca)*. Yale Univ., Peabody Mus.Nat.Hist.Bull.*22*, 1–140.

MANO, K., and OMORI, M. (1969): *Microsopic Structure of Hinge Teeth in Taxodonta, Lamellibranchia*. Part I. *The Hinge Teeth Structure of the Genus Anadara*. Venus, Jap.J.Malacol.*27*, 141–152.

NATHUSIUS-KÖNIGSBORN, W. VON (1877): *Untersuchungen über nichtcelluläre Organismen, namentlich Crustacean-Panzer, Mollusken-Schalen und Eihüllen*, Berlin, 144 p. (*Fide* MACCLINTOCK 1967).

NEWELL, N.D. (1937): *Late Paleozoic Pelecypods; Pectinacea*. Kan.Geol.Surv.Rept. [Part 2] *10*, 1–123.

– (1969): *Classification of Bivalvia:* in: MOORE, R.C., Ed., *Treatise on Invertebrate Paleontology* [Part N], Mollusca 6 (Bivalvia), p.205–218.

OBERLING, J.J. (1955): *Shell Structure of West American Pelecypoda*. J. Wash. Acad. Sci. *45*, 128–130.

– (1964): *Observations on Some Structural Features of the Pelecypod Shell*. Mitt.Naturf.Ges.Bern [N.F.] *20*, 1–63.

OMORI, M., and KOBAYASHI, I. (1963): *On the Micro-Canal Structure Found in the Shell of Arca navicularis Bruguière and Spondylus barbatus Reeve*. Venus, Jap.J. Malacol.*22*, 274–280.

OMORI, M., KOBAYASHI, I., and SHIBATA, M. (1962): *Preliminary Report on the Shell Structure of Glycymeris vestita (Dunker)*. Sci.Rep.Tokyo Kyoiku Daig. [Sec.C] *8*, 197–202.

RHEYNE, A. (1951): *On the Structure of the Shells and Pearls of Tridacna squamosa Lam. and Hippopus hippopus (Linn.)*. Archs néerl.Zool.*8*, 206–241.

SCHMIDT, W.J. (1923): *Bau und Bildung der Perlmuttermasse*. Zool.J., Abt.Ontog.Tiere *45*, 1–148.

SHIBATA, M. (1965): *On the Conchiolin Structure of Glycymeris vestita (Dunker)*. Earth Sci. (Chikyu Kagaku) *81*, 13–16.

TAYLOR, J.D., and KENNEDY, W.J. (1969): *The Shell Structure and Mineralogy of Chama pellucida Broderip*. Veliger *11*, 391–398.

TAYLOR, J.D., KENNEDY, W.J., and HALL, A. (1969): *Shell Structure and Mineralogy of the Bivalvia: (Nuculacea-Trigonacea)*. Bull.Br.Mus.nat.Hist., Zoology, suppl.*3*, 125 p.

THIELE, J. (1893): *Beiträge zur Kenntnis der Mollusken. II. Über die Molluskenschale.* Z. wiss. Zool. *55*, 220–251.

TRUEMAN, E. R. (1942): *The Structure and Deposition of the Shell of Tellina tenuis.* J. R. microsc. Soc. *62*, 69–92.

TULLBERG, T. (1882): *Studien über den Bau und das Wachstum des Hummerpanzers und der Molluskenschalen.* K. Svensk. Vetensk. Akad. Handl. Stockholm. *19*, 1–57.

WISE, S. W. (1969a): *Ultrastructure of the Molluscan Crossed Lamellar Layer.* Abs., Geol. Soc. Am. Sp. Paper *87*, 187–188.

– (1969b): *Study of Molluscan shell Ultrastructures*, in: JOHARI, O., Ed., *Scanning Electron Microscopy 1969*, Illinois Inst. Technology Research Inst., Chicago, p. 205–216.

– (1970): *Microarchitecture and Mode of Formation of Nacre (Mother-of-Pearl) in Pelecypods, Gastropods, and Cephalopods.* Eclogae geol. Helv. *63*/3, 775–797.

WISE, S. W., and HAY, W. W. (1968a): *Scanning Electron Microscopy of Molluscan Shell Ultrastructures. I. Techniques for Polished and Etched Sections.* Trans. Am. microsc. Soc. *87*, 411–418.

– (1968b): *Scanning Electron Microscopy of Molluscan Shell Ultrastructures. II. Observations of Growth Surfaces.* Trans. Am. microsc. Soc. *87*, 419–430.

WISE, S. W., STIEGLITZ, R. D., and HAY, W. W. (1970): *Scanning Electron Microscope Study of Fine Grain Size Biogenic Carbonate Particles.* Trans., Gulf Coast Assoc. Geol. Socs. *20*, 287–302.

Plate I

Fig. 1 — *Anadara notabilis* (RÖDING). Light micrograph, exterior of left valve. Bristle-like covering is periostracum 1.5 ×. All subsequent micrographs in this report are of *A. notabilis* with the exception of Textfigure 2.

Fig. 2 — Light micrograph of interior of left valve showing position of the pallial line (arrow *PL*) and the developmental growth surfaces of the principal shell deposits: myostracum or muscle deposits (*M*); complex crossed lamellar layer (*CPX*, interior [darker] portion of the shell inside the pallial line); and crossed lamellar layer (*CL*, lighter colored and ribbed margin of the shell outside the pallial line). White line indicates trace of radial section shown in Figure 3 (below), 1.2 ×.

Fig. 3 — Radial section cut along white line indicated in Figure 2 (above) showing relative positions of the inner (*CPX*, complex crossed lamellar) and outer (*CL*, crossed lamellar) shell layers. Myostracum and ligament deposits not shown. This and succeeding micrographs of shell layers are oriented with inner layer at top of figure, 1.5 ×.

Fig. 4 — Radial fracture section intersecting inner surface of shell (*IS*) exposing a thin myostracum (*M*) overlying the crossed lamellar layer (*CL*). The long vertical sheet-like units of the crossed lamellar layer are first order lamels. These are always oriented perpendicular to the growth surface of the layer and are composed of finer elements which, in adjacent lamels, are inclined in opposite directions. 200 ×.

Fig. 5 — View of inner surface along ventral margin of specimen shown in Figure 2. Pallial line (arrow *PL*) separates inner layer (top half of figure) from crossed lamellar layer (lower half). The inner layer is marked by numerous linear grooves and ridges which extend from the pallial line toward the beak. The grooves are punctuated by numerous small tubules. Traces of first order lamels are visible on the growth surface of the crossed lamellar layer parallel to the ventral margin, 80 ×.

Fig. 6 — Growth surface of crossed lamellar layer, lightly etched to show finer elements of four first order lamels. The finer elements of adjacent first order lamels are inclined at the same angle but in opposite directions to the growth surface, 2,100 ×.

Fig. 7 — Detail of a portion of Figure 6 (above) showing the boundary between two first order lamels, 5,000 ×.

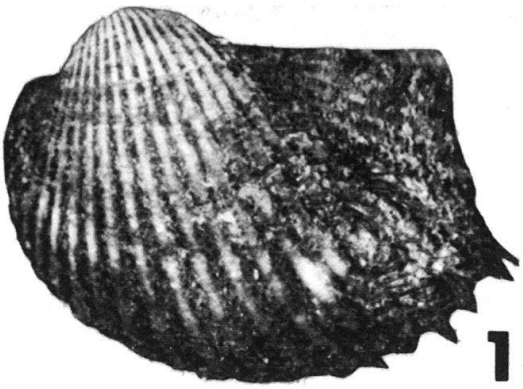

1

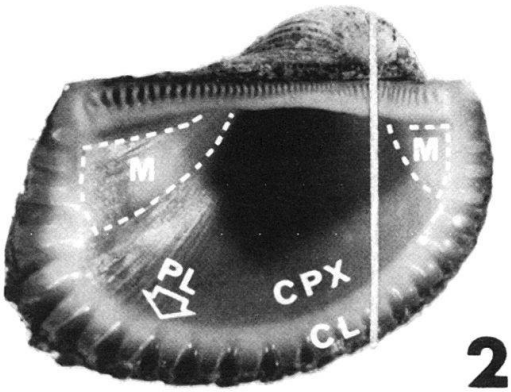

2

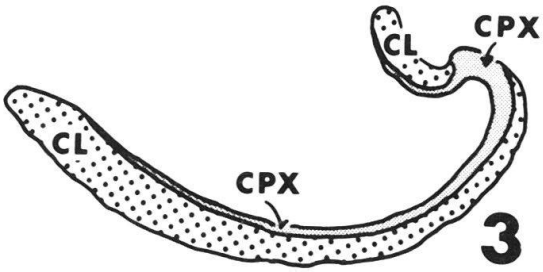

3

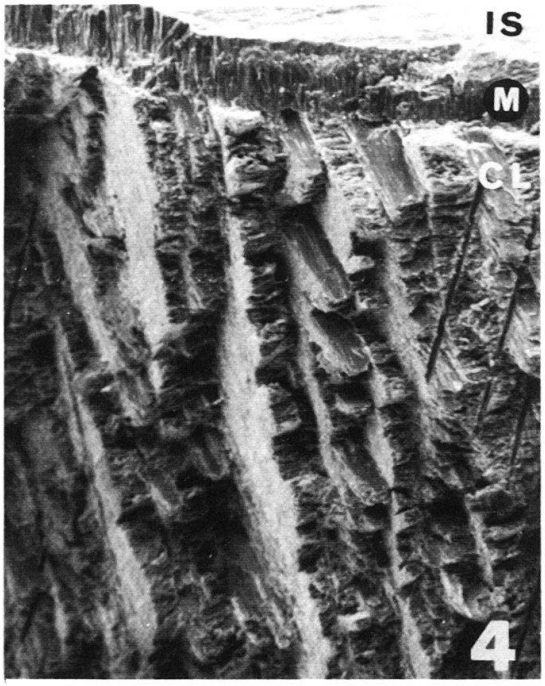

4

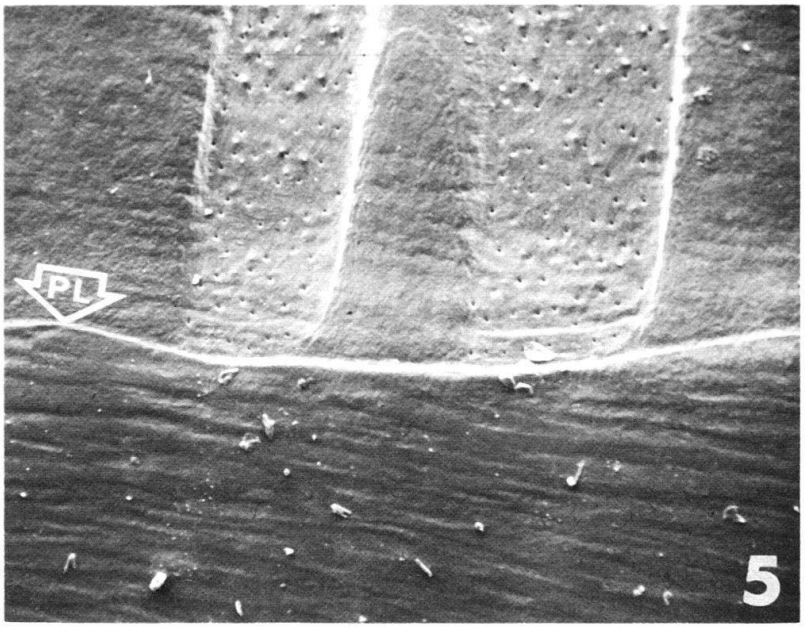

5

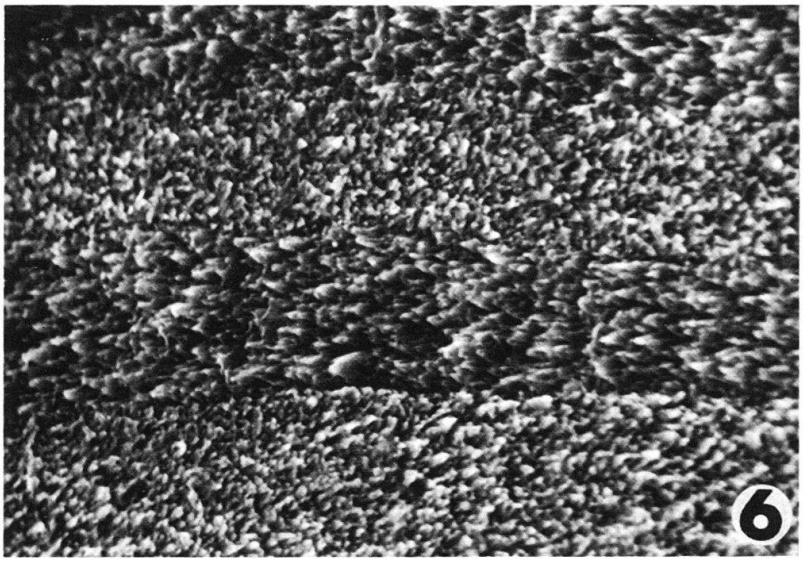

6

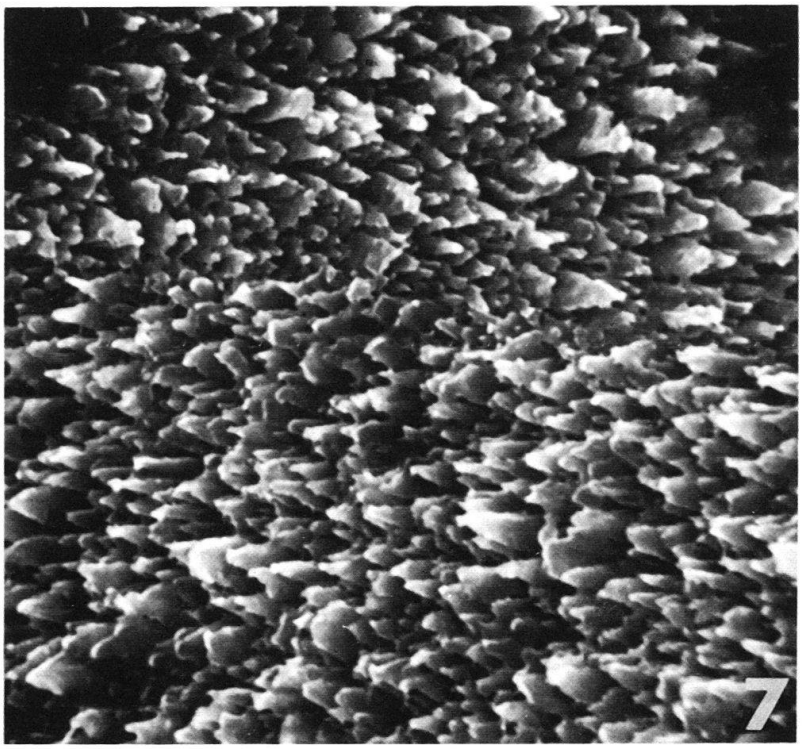

7

Plate II

Fig. 1 Transmission electron micrograph of etched, polished section cut nearly parallel to the growth surface of crossed lamellar layer, showing two first order lamels. Etch pattern suggests that the finest elements shown are laths approximately 0.5 μ wide, 11,000 ×.

Fig. 2 Radial fracture intersecting growth surface of crossed lamellar layer. First order lamels are outlined by slight depressions on growth surface; fracture reveals the opposed inclinations of finer elements of the lamels, 900 ×. (WISE et al. 1969).


1

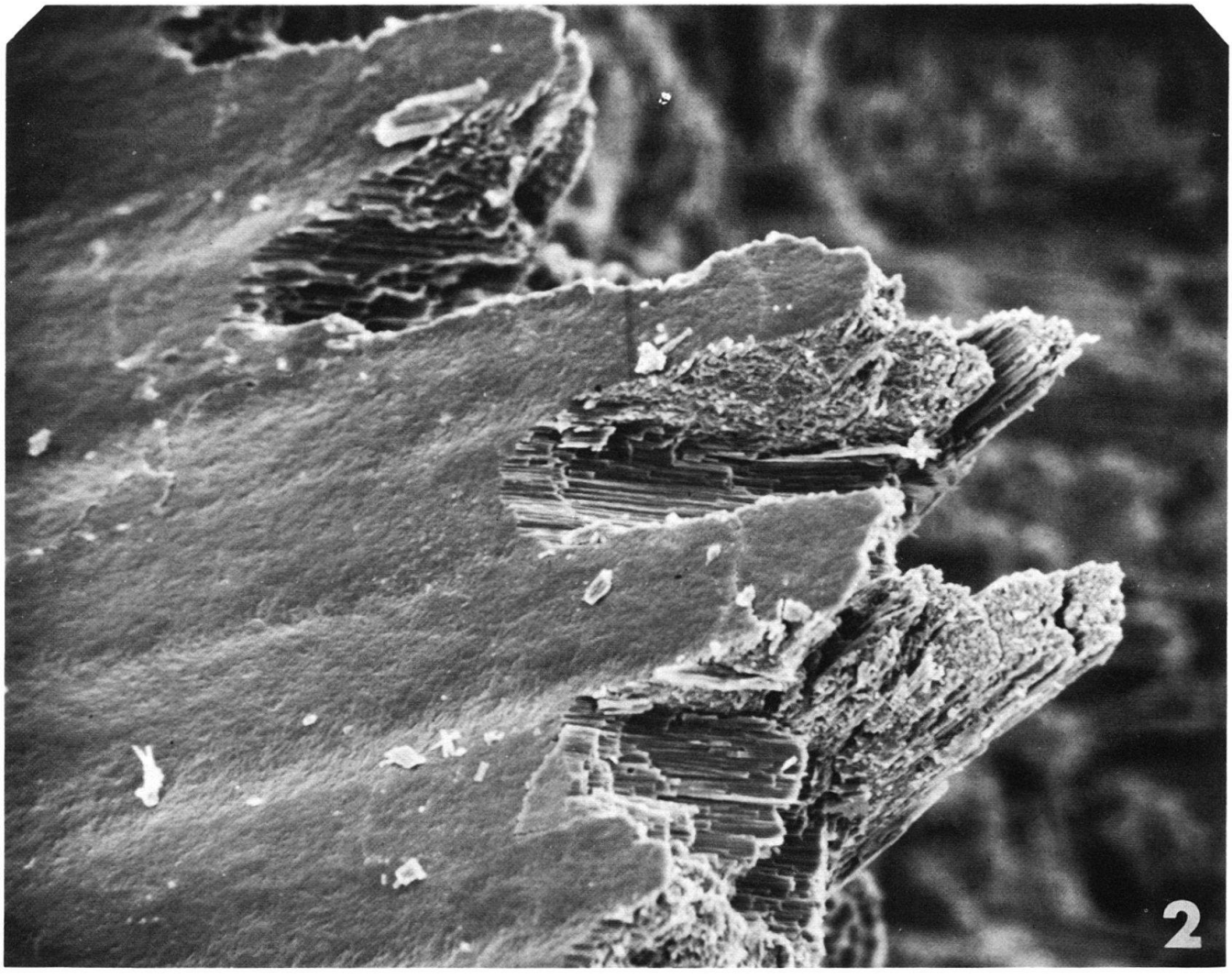
2

Plate III

Fig. 1 Transmission electron micrograph of an etched polished section cut parallel to the plane of a first order lamel revealing the true thicknesses of the third order lamels, 13,000 ×.

Fig. 2 Radial fracture following the plane of inclination of one set of second order lamels but truncating the alternate set at right angles, 240 ×.

Fig. 3 View perpendicular to the fracture shown in Figure 2 (above). Second order lamels in the truncated set appear as lath shaped stubs, 1,200 ×.

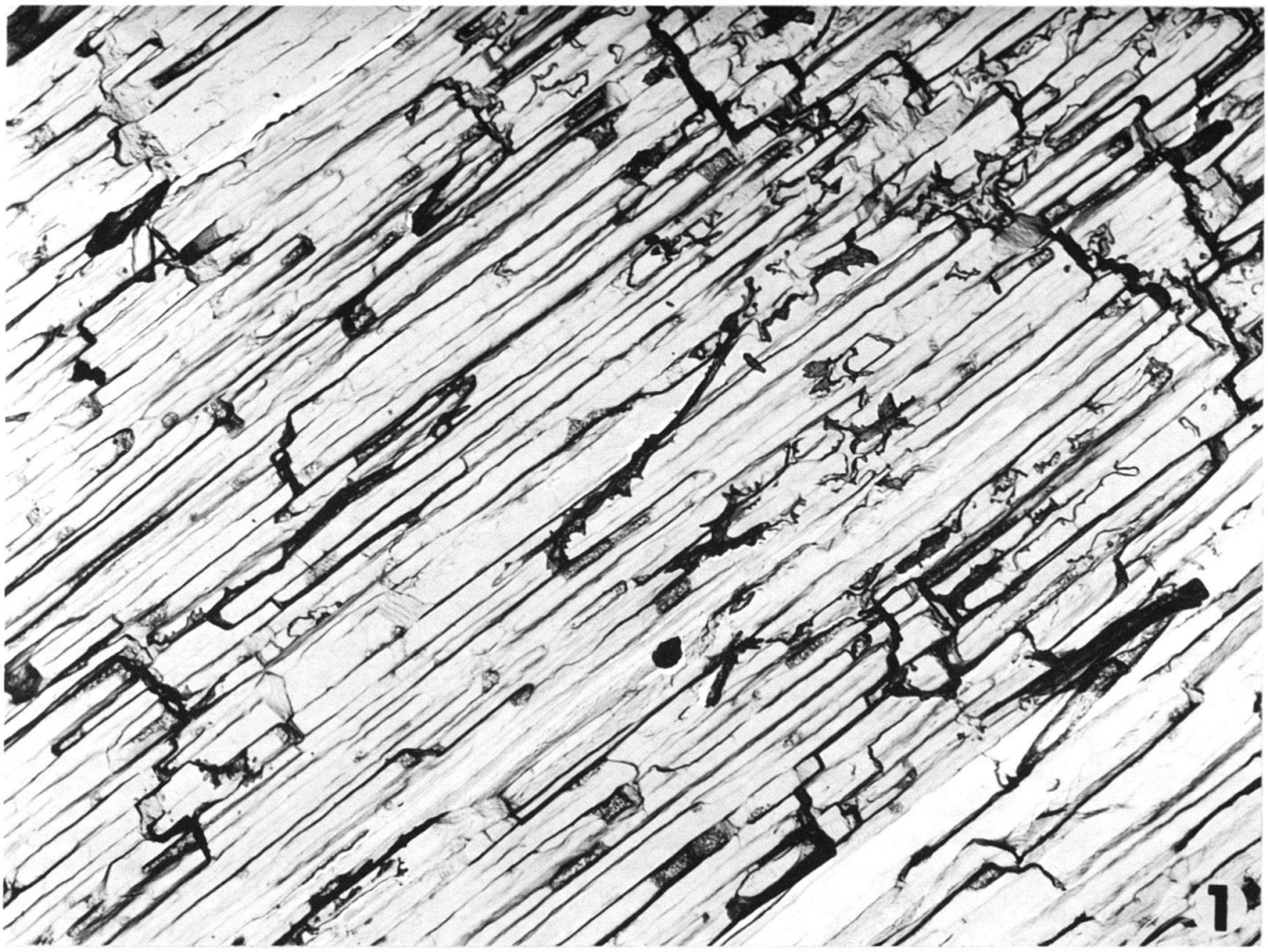
1

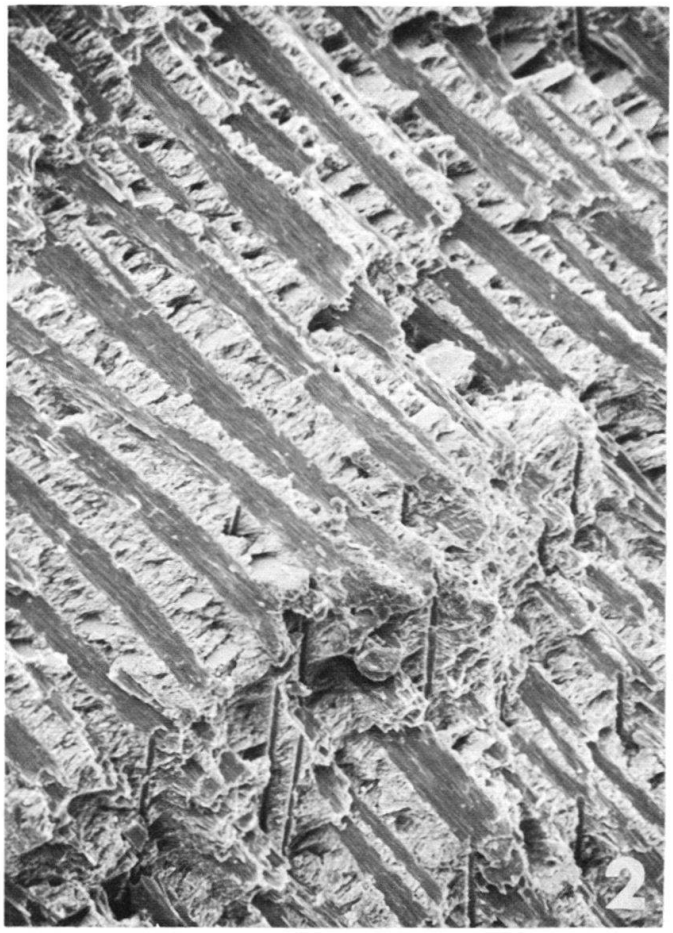
2


3

Plate IV

Fig. 1 Diagram showing orientation of a radial shell section (*R*) through a set of concentrically oriented first order lamels. Second order lamels appear as parallel horizontal traces on the section.

Fig. 2 Light micrograph of a cellulose acetate peel of a polished and etched radial section showing arrangement of first order lamels (vertical units) and second order lamels (horizontal traces) predicted from diagram in Figure 1, 220 ×.

Fig. 3 Acetate peel from an etched polished section showing complex crossed lamellar layer (above) and crossed lamellar layer (below). Arrow points to wedge of myostracum. First order lamels of upper half (proximal portion) of the crossed lamellar layer are parallel and only slightly curved while those of lower half (in the area where ribs are formed) have a predominantly horizontal orientation.
Faint white streaks slanting through crossed lamellar layer to the left are growth lines, 11 ×.

Fig. 4 Scanning electron micrograph of a portion of the section in Figure 3 (above). Long straight parallel first order lamels in proximal portion of crossed lamellar layer (upper third of figure) change abruptly to short, interwoven, anastomosing and bifurcating units in ribbed region of shell (lower two-thirds of figure), 60 ×.

Fig. 5 Transverse fracture (perpendicular to ribs) showing complexities of ribbed portion of shell (proximal direction toward bottom of figure). Horizontal first order lamels follow contours of ribs, 180 ×.

Fig. 6 View of ribbed area at higher magnification. Despite complexities in this area of shell, the characteristic opposed inclination of second order lamels in adjacent first order lamels is discernible, 590 ×.

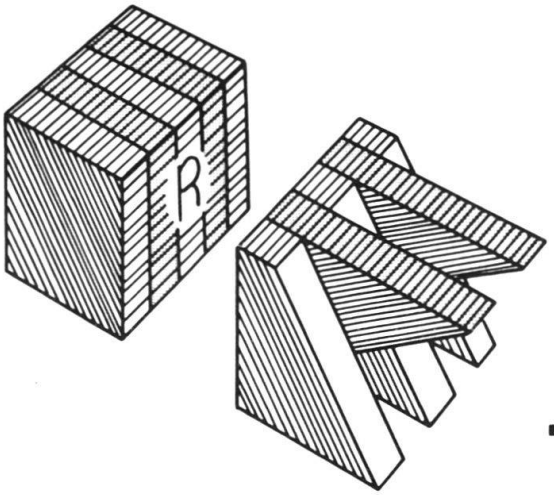

1

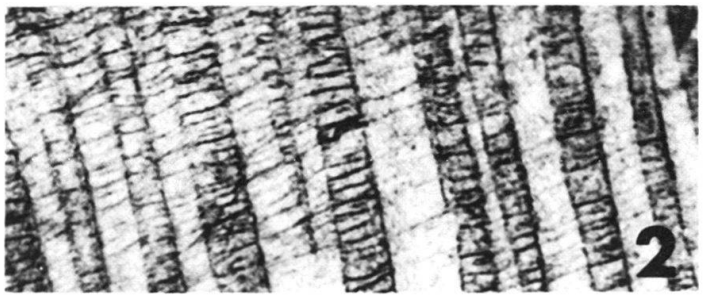

2

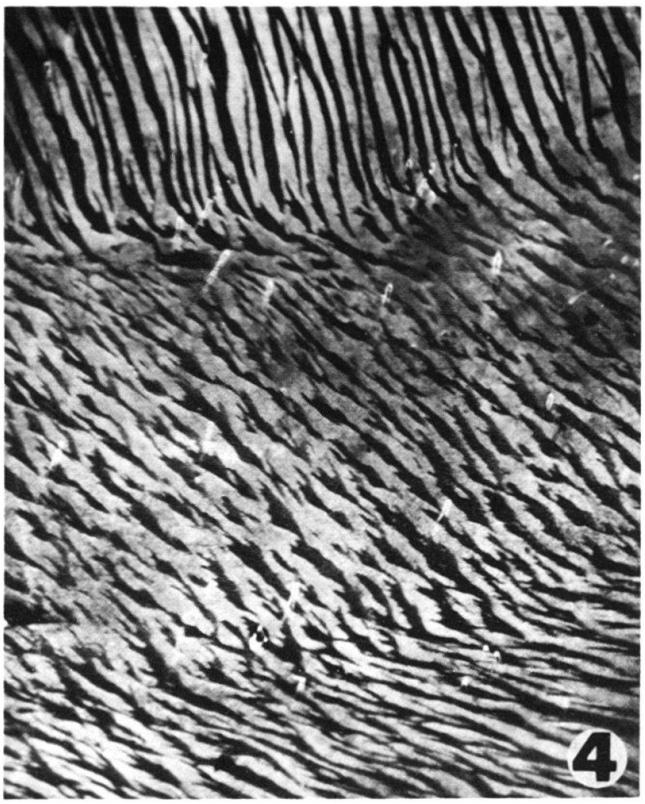

4

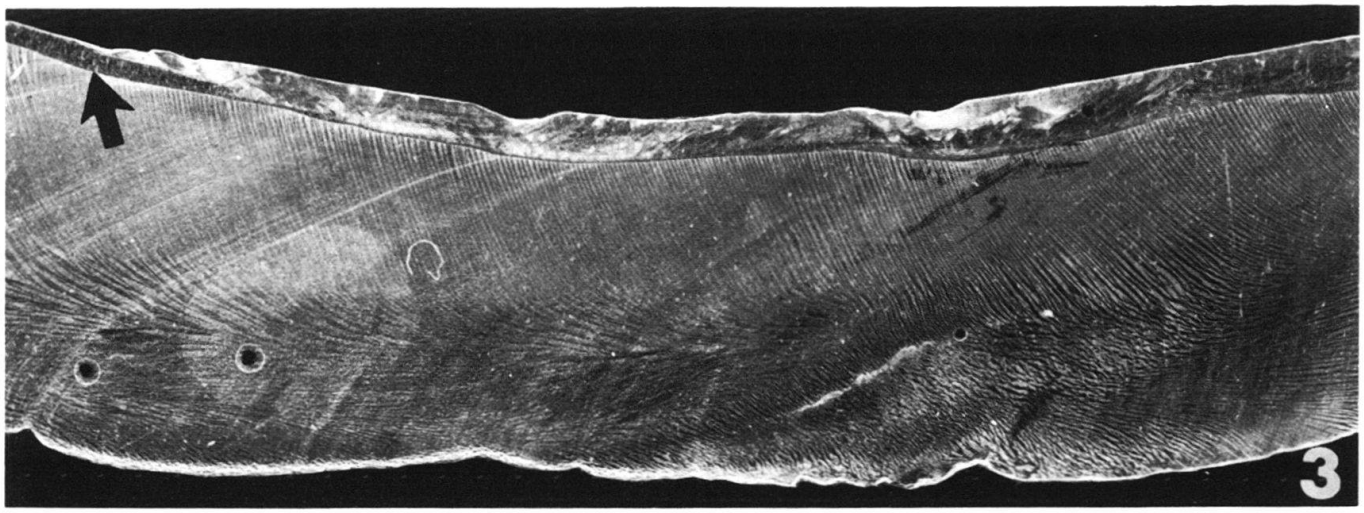

3

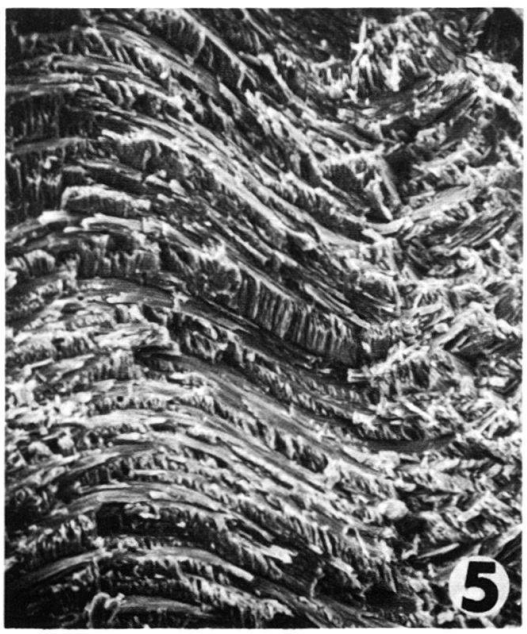

5

6

Plate V

Fig. 1 Groove on surface of inner layer originating at the pallial line. Tubules are emplaced just inside the pallial line; the last ones formed are aligned in an arcuate row, 240 ×.

Fig. 2 and 3 Radial fracture surface intersecting inner shell surface showing ralationship between tubules and mineral layers of the shell. 2. Portions of two rows of tubules seen in grooves transversing inner surface from left to right. Tubules are formed in the crossed lamellar layer and penetrate it to the periostracum. They are inclined toward the ventral margin at about a 70° angle to the inner shell surface, 200 ×. 3. As the complex crossed lamellar layer is deposited around them, the tubules remain open, maintaining an orientation perpendicular to the inner layer, 200 ×.

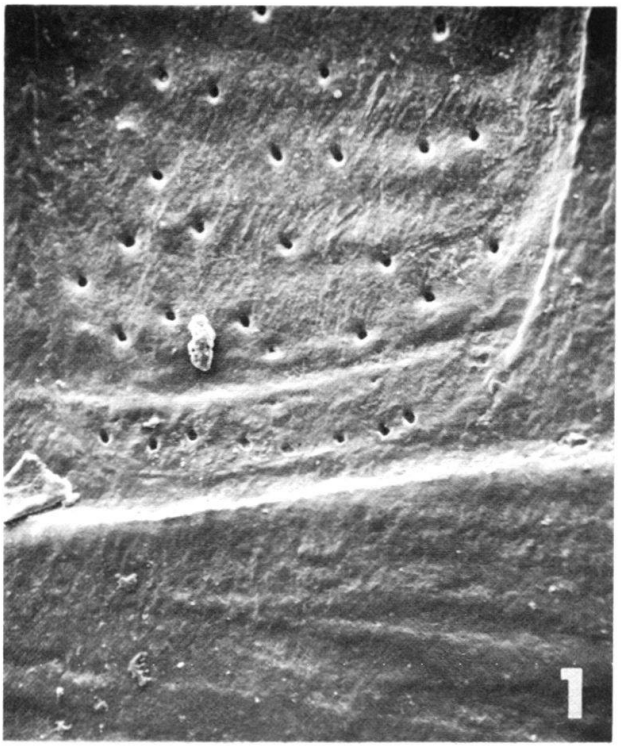
1

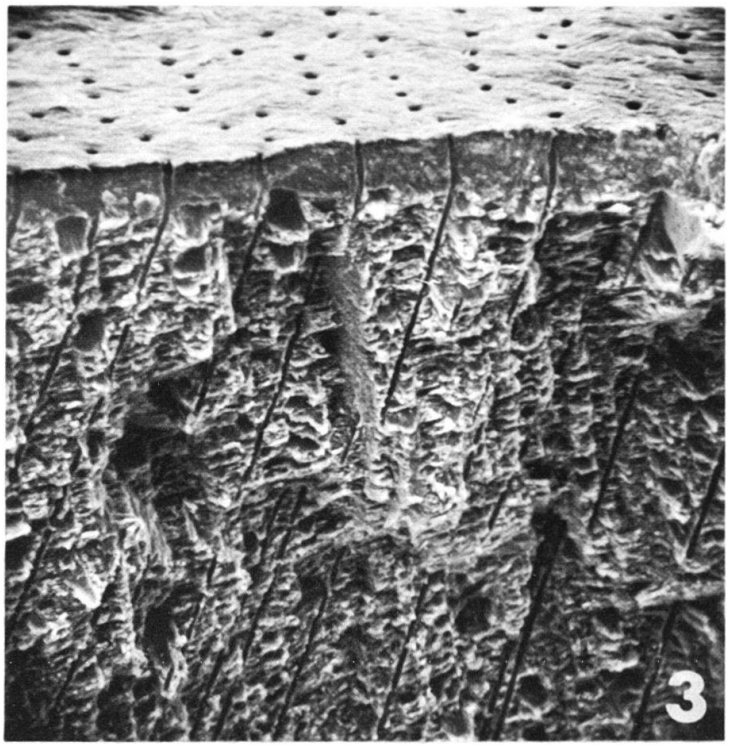
3


2

Plate VI

Fig. 1 and 2 — Tubule openings partially filled by unidentified organic material. 1. 3,200×; 2. 5,000×.

Fig. 3 — View of inner shell surface looking toward the ventral margin; crossed lamellar layer and pallial line at top of figure. Grooves punctuated by tubules (*T*) are separated by ridges composed of myostracum (*M*) and run from the pallial line toward beak, 23×.

Fig. 4 — Surface of a tubulate groove. Complex crossed lamellar layer is deposited as long strands of aragonite aligned in a linear pattern which runs subparallel to the length of the groove. The surface is marked by small bumps which often form around tubule openings, 290×.

Fig. 5 — Close-up of the area enclosed by white rectangle in Figure 3 (above) showing dorsal termination of a myostracum ridge (*M*, center of figure). Toward the beak, ridges between the tubulate grooves become covered by deposition of the complex crossed lamellar layer. Over the ridges strands of aragonite forming the complex crossed lamellar layer are deposited in a reticulate cross-matted pattern (*CM*) instead of in the smoothly lineated pattern developed in the grooves, 125×.

Fig. 6 — Boundary between groove and ridge showing aragonite strands forming a lineated pattern (*L*) around tubules of groove (left) and a cross-matted pattern over the ridge (right), 590×.

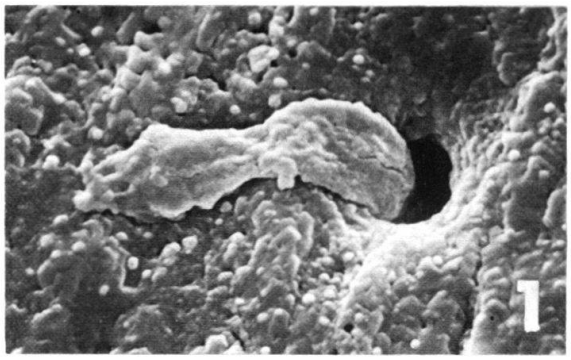
1

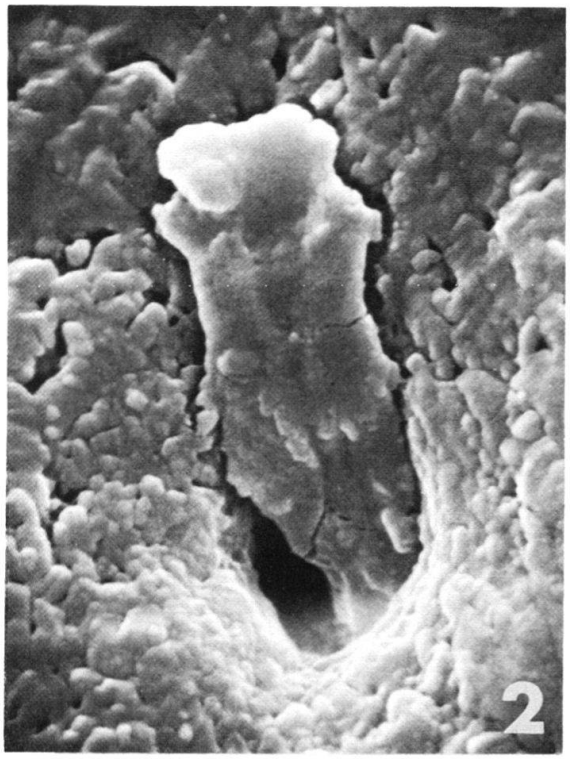
2

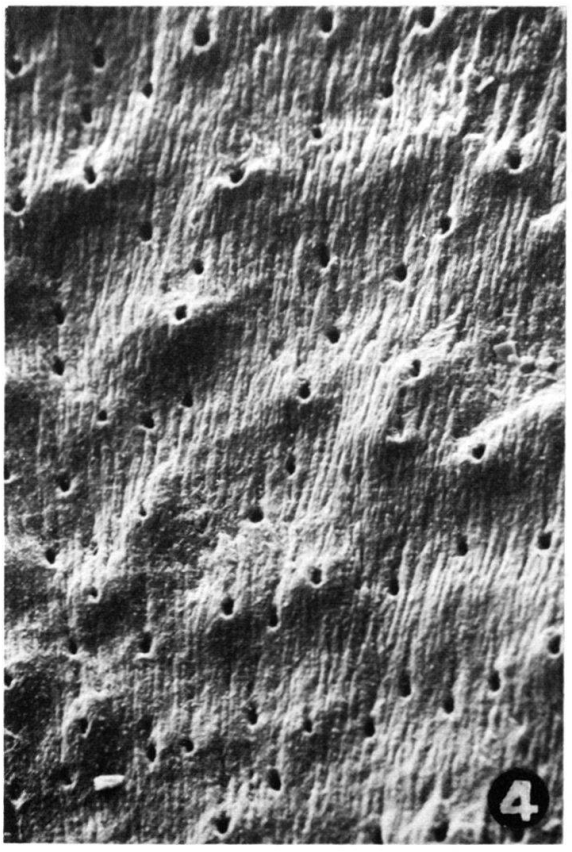
4

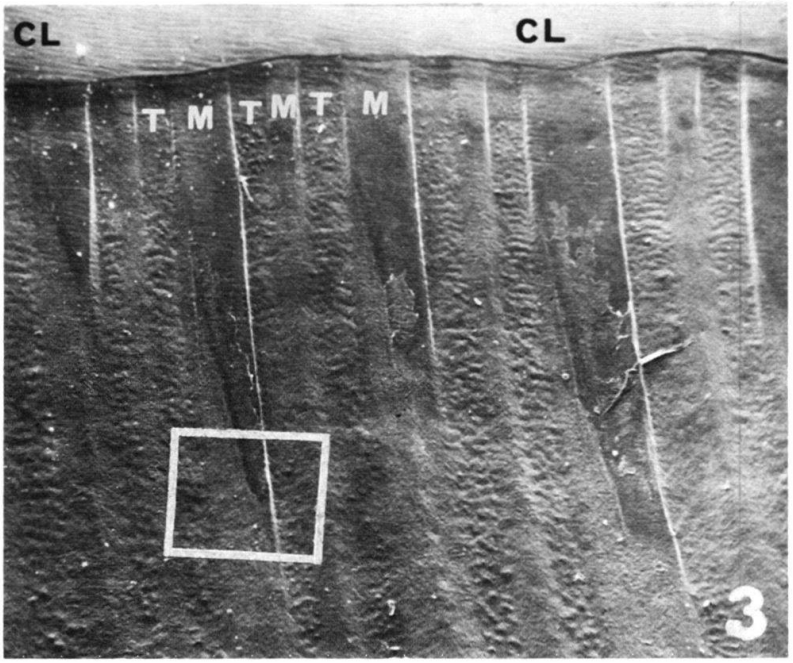
CL
CL
T M T M T M
3

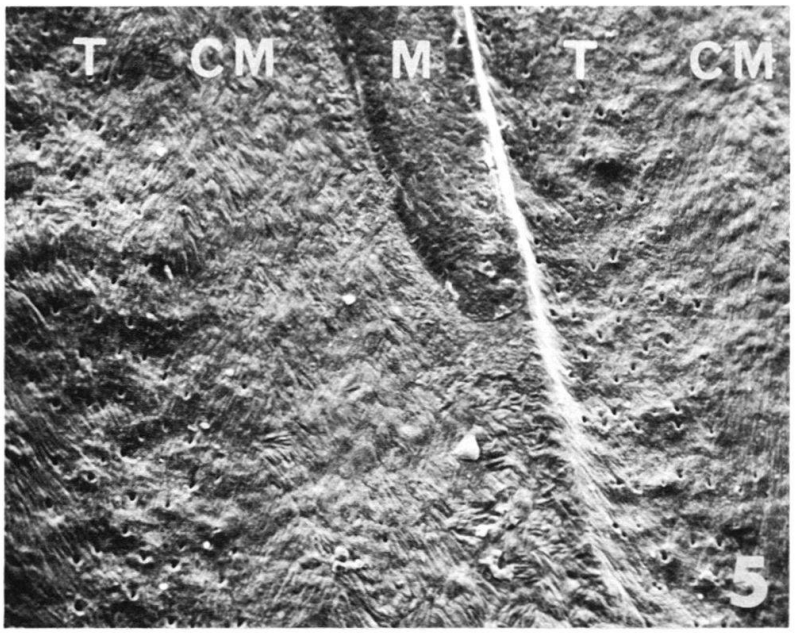
T CM M T CM
5

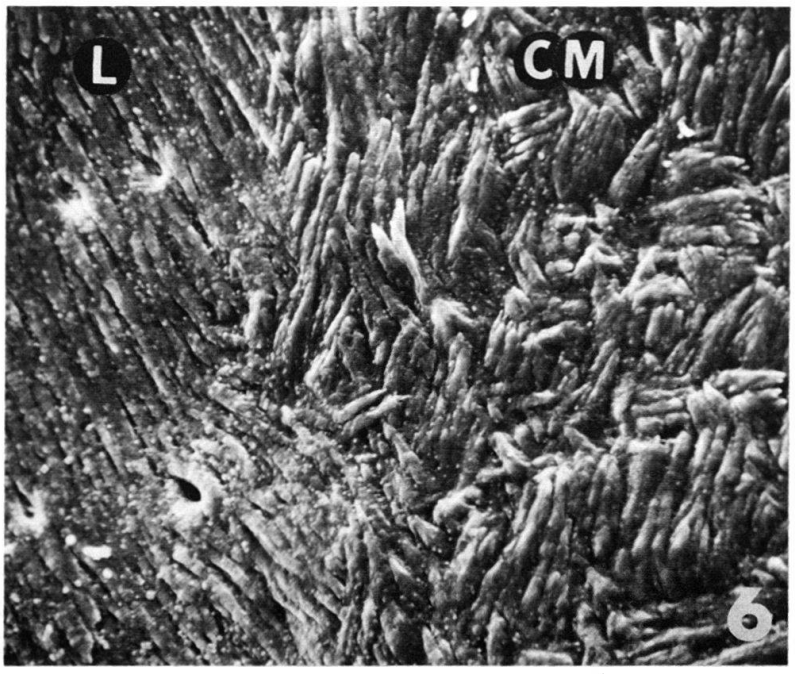
L
CM
6

Plate VII

Fig. 1 Radial fracture section intersecting inner shell surface showing the tubulate surface of a groove (upper third of figure) floored by lineated strands of the complex crossed lamellar layer (*CPX*). Below complex crossed lamellar layer are vertical first order lamels of the crossed lamellar layer (*CL*), 690 ×.

Fig. 2 Transverse fracture surface intersecting inner shell surface. Turbulate grooves and ridges of myostracum form a veneer over the prominent crossed pattern of the crossed lamellar layer. This micrograph clearly demonstrates that tubules penetrate grooves instead of ridges, 280 ×.

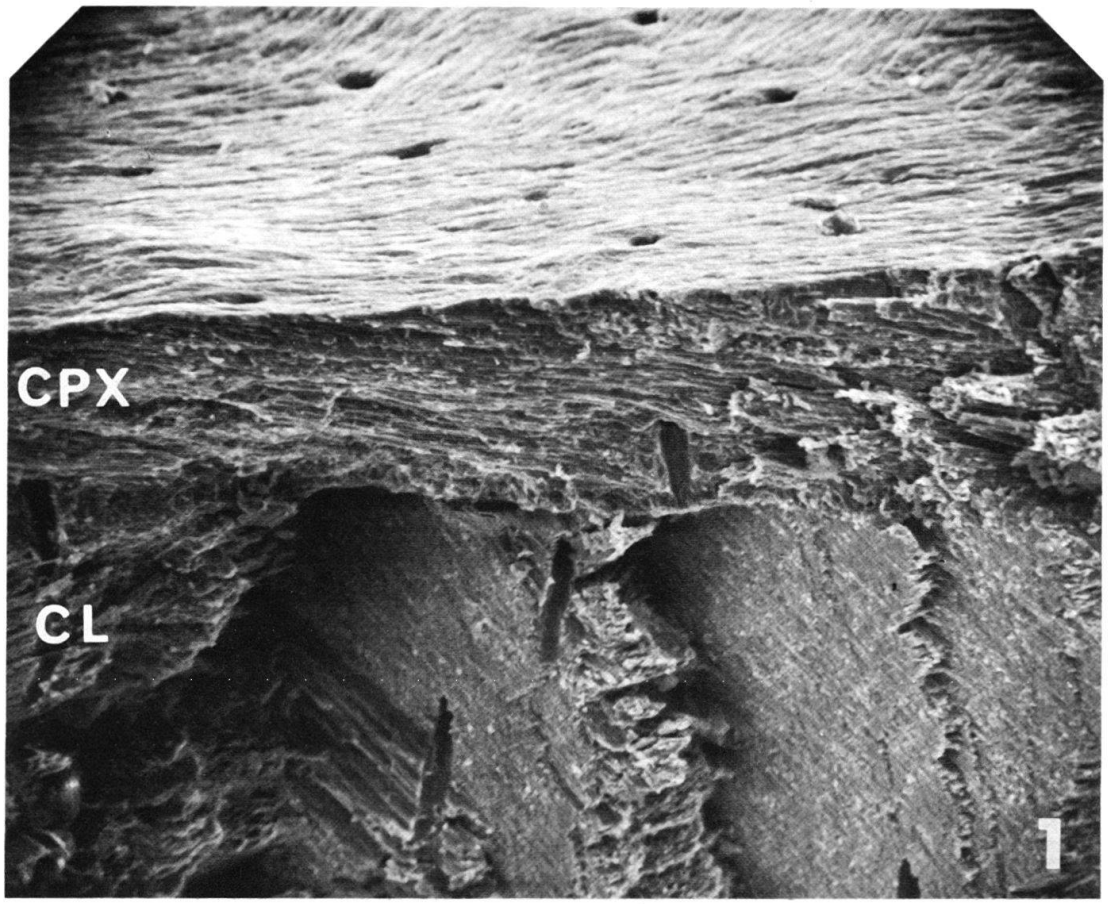
CPX
CL
1


2

Plate VIII

Fig. 1 Fracture through a ridge reveals the prismatic structure of the myostracum, 1,600 ×.

Fig. 2 Surface of myostracum forming ridges covered by a thick organic membrane. Arrow points to a crack in this mat-like covering, 1,400 ×.

Fig. 3 Fracture through myostracum deposited by posterior adductor muscle, 260 ×.

Fig. 4 Acetate peel of transverse section through shell showing 1. bifurcating structure of lamels in the ribs (*R*; lable *I* marks a rib interspace) and 2. myostracum deposits of ridges of the inner layer (arrows), 16 ×.

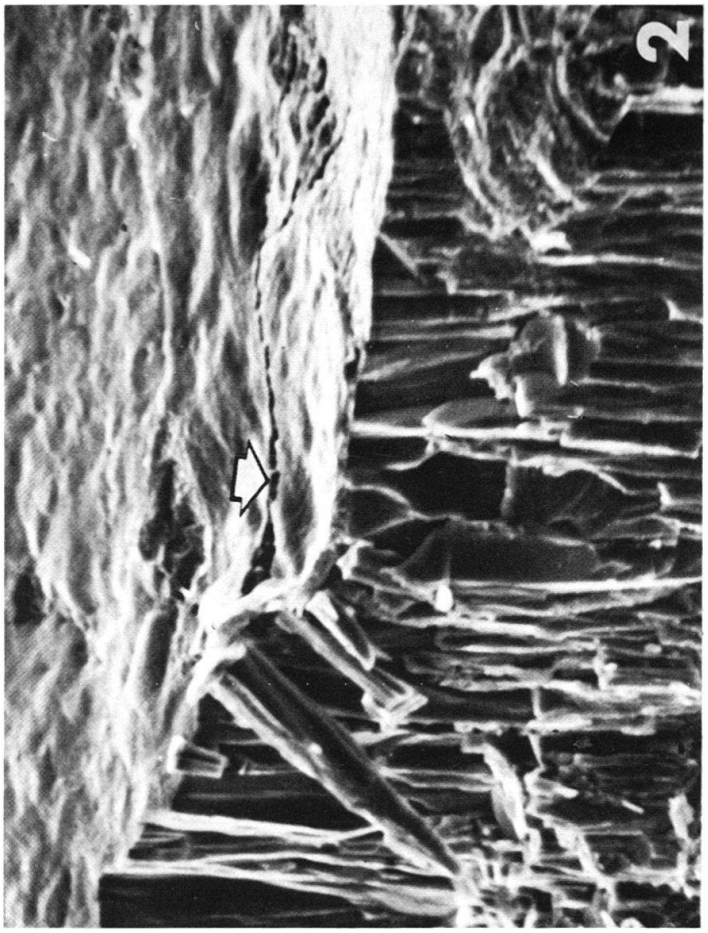
2

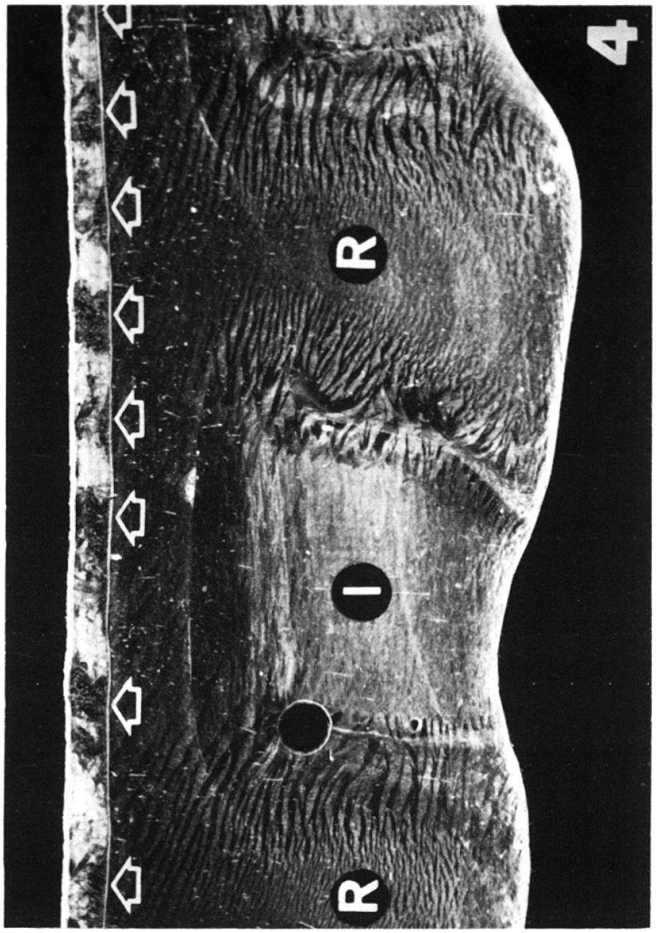
4
R
I
R

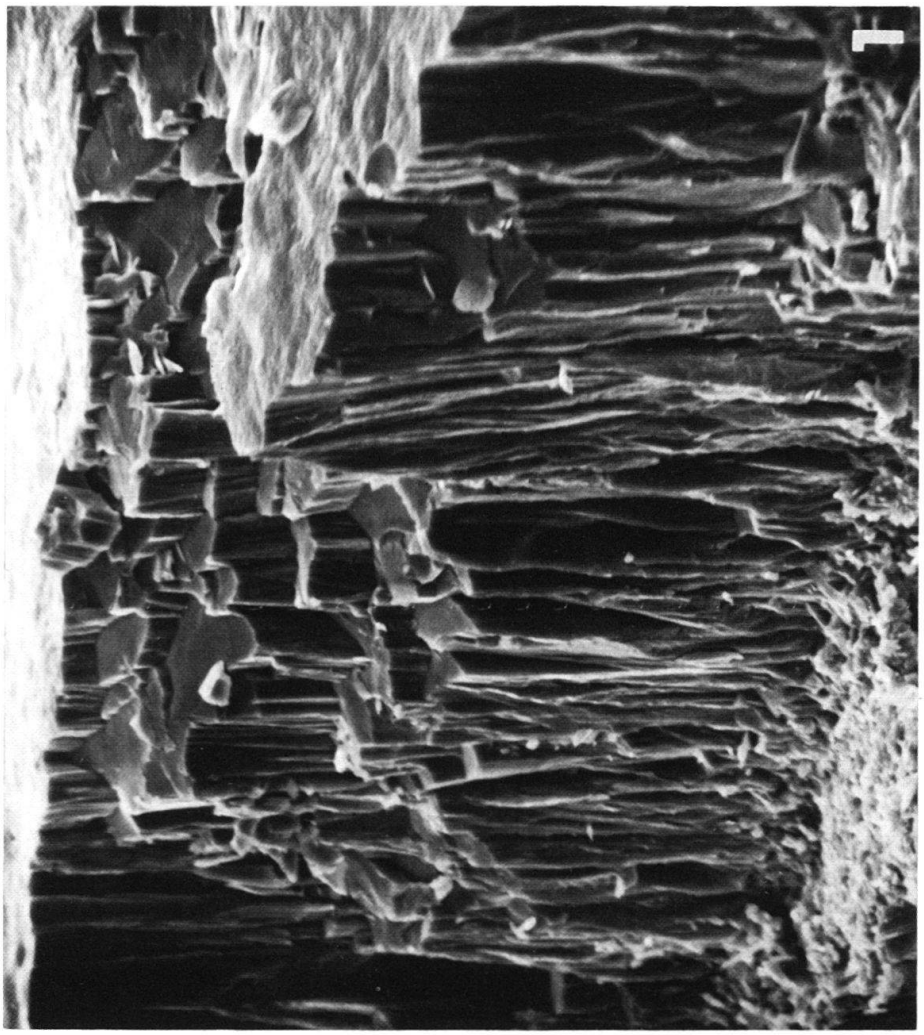
1

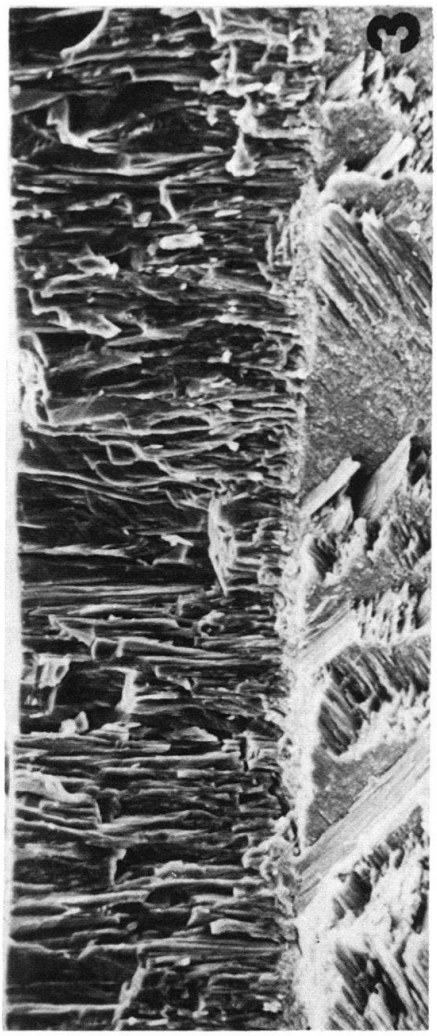
3

Plate IX

Fig. 1 Radial section (polished and etched 2 minutes in 1.0% HCl solution) through the complex crossed lamellar layer (*CPX*), a myostracum ridge (*M*), and the proximal portion of the crossed lamellar layer. Ventral direction indicated by arrow *V*. Fig. 2–5 show details of this section.

Fig. 2 Lineated structure of complex crossed lamellar layer, 2,000 ×.

Fig. 3 Irregularities of structure in complex crossed lamellar layer, 1,000 ×.

Fig. 4 Wedge-shaped prisms of myostracum, 1,100 ×.

Fig. 5 Stereo pair of myostracum showing vertical wedge-shaped prisms overlying substructure of units inclined toward dorsum; complex crossed lamellar layer above, 900 ×.

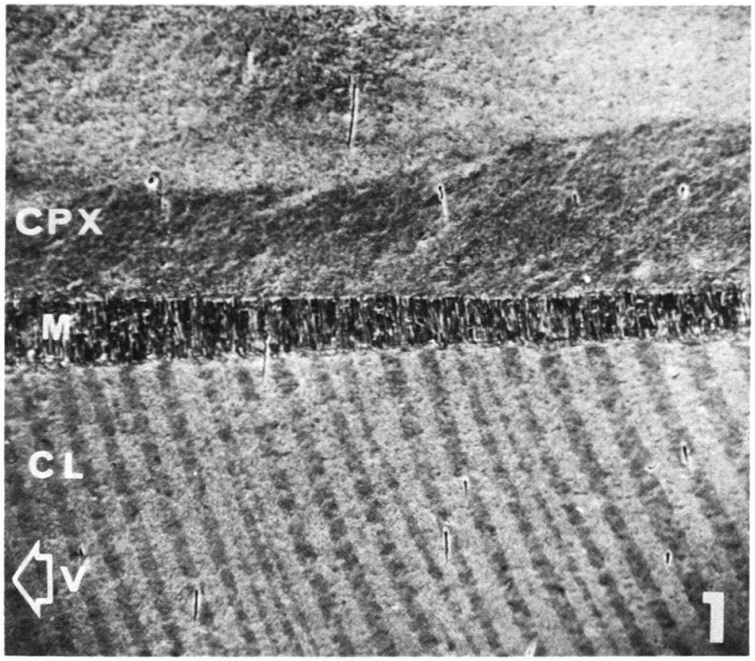
CPX
M
CL
V
1

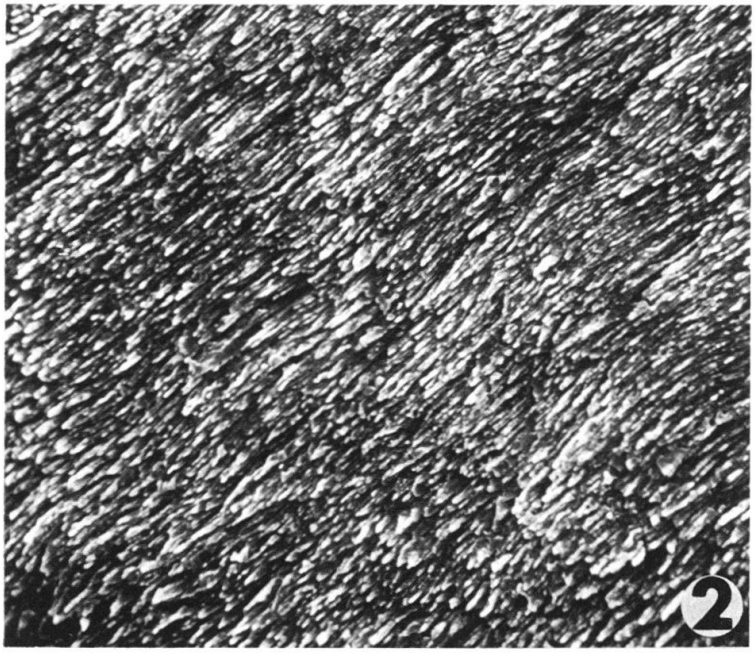
2

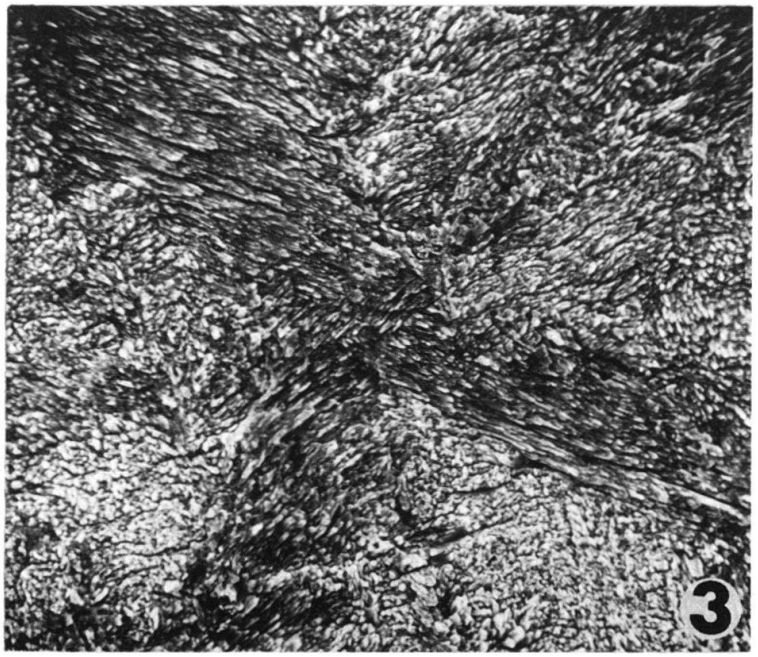
3

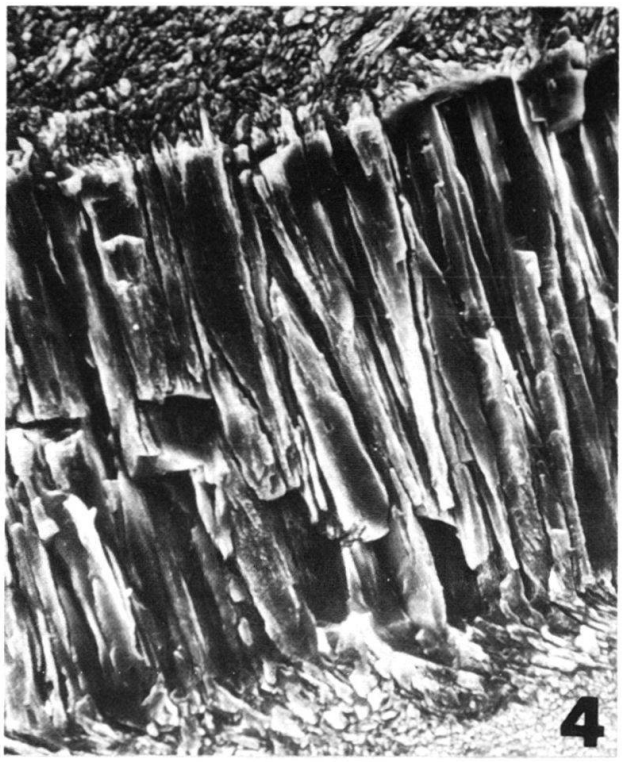
4

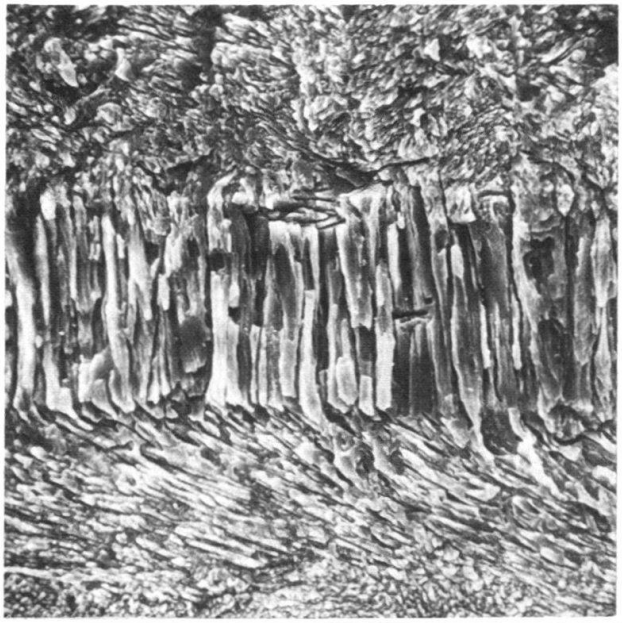

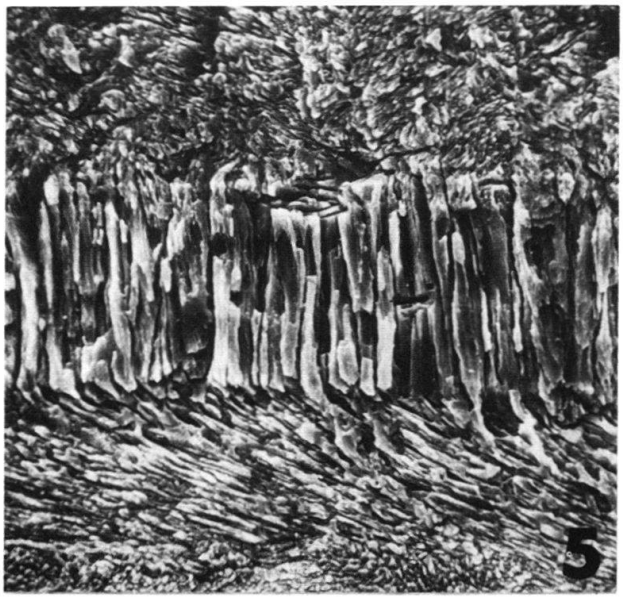
5